Accelerating Synchrotron-Based Characterization of Solar Materials: Development of Flyscan Capability

Ashley E. Morishige[1], Hannu S. Laine[2], Mallory A. Jensen[1], Patricia X. T. Yen[1], Erin E. Looney[1], Stefan Vogt[3], Barry Lai[3], Tonio Buonassisi[1]

[1]Massachusetts Institute of Technology, Cambridge, MA 02139, USA, email: aemorish@alum.mit.edu
[2]Department of Micro and Nanosciences, Aalto University, Tietotie 3, 02150 Espoo, Finland
[3]Advanced Photon Source, Argonne National Laboratory, Argonne, IL 60439, USA

Abstract — **Synchrotron-based μ-XRF is a powerful tool to measure elemental distributions non-destructively with high spatial resolution (<200 nm) and excellent sensitivity (typically ~10^{14} atoms/cm^{-2}). Recently, we implemented on-the-fly data collection (flyscan) at Beamline 2-ID-D at the Advanced Photon Source at Argonne National Laboratory, making data acquisition faster than 300 ms per pixel practical. We show that flyscan mode at Beamline 2-ID-D enables (a) traditional elemental maps to be completed twenty times more quickly while maintaining reasonably high sensitivity, and (b) practical studies of materials with an order of magnitude lower total impurity concentration and sparser spatial density of impurities. We highlight opportunities for flyscan to enable qualitatively new forms of microscopy, leveraging the accelerated data-acquisition rate for multi-dimensional mapping (*e.g.*, depth, rotation, temperature, bias voltage).**

I. Introduction

Synchrotron-based micro-X-ray fluorescence spectroscopy (μ-XRF) is a spatially resolved, non-destructive, sensitive, and relatively large-area spectroscopy technique that can be used to map elemental distributions in materials. This technique has been used to characterize and develop improved impurity-gettering processes for multiple detrimental metal species in several different PV-Si materials [1-3]. Given a specified time spent collecting fluorescence in a given pixel (dwell time), the local concentration of an element must be high enough to be detected, and particles must be at a high enough spatial density so a particle can be detected within a practical scan area. For this work, a typical high-resolution μ-XRF scan is defined as having a 1000 ms dwell time, a 220 nm step size, and taking 8 hours to complete.

During μ-XRF acquisition, a sample is mounted on an *x-y* sample stage. One of two data-collection modes is used: step-by-step (stepscan) or on-the-fly (flyscan) [4]. Stepscan mode involves settling time at each pixel, which increases measurement overhead. During flyscan, the motors move continuously and time intervals define the bounds of each pixel. In stepscan mode at Argonne National Laboratory's Advanced Photon Source beamline 2-ID-D, the typical overhead time is ~300 ms per pixel. Flyscan avoids this overhead time, enabling practical use of dwell times shorter than 300 ms. This time saving translates into faster scanning of typical samples compared to a typical 1000 ms dwell time, 30% larger map sizes within the same scan time without sacrificing sensitivity, or orders of magnitude larger map sizes if sensitivity or step size requirements can be relaxed. This increase in efficiency is critical to faster cycles of learning and increased productivity of limited, expensive, complex user facility resources, where a typical user has access to the tool for only a few days a year.

An open question with this new flyscan capability is the tradeoff between dwell time and sensitivity. Scanning larger areas more quickly is beneficial, but it is essential to maintain adequate sensitivity to the element distribution of interest. In multicrystalline silicon, recombination-active metal impurities in parts per billion are found in point defect and precipitated forms [5–10], so both types of defect must be controlled during solar cell processing to maximize cell performance. In this benchmarking study, using five different dwell times, we measure the same region of a previously well-characterized *n*-type multicrystalline silicon sample containing trace amounts of iron, and we quantify the decrease in sensitivity as dwell time is reduced. Additionally, using results from an established simulation tool [11], we show that with flyscans, it is practical to measure silicon with lower total impurity concentrations and a lower density of impurity particles using μ-XRF in flyscan mode.

II. Methods

Multicrystalline *n*-type 2 Ω-cm silicon wafers were obtained from an industrial directionally solidified Gen5 ingot. A 1×1 cm^2 sample containing a Σ33 grain boundary identified by electron backscatter diffraction was selected from the low-lifetime border region of a wafer from a corner brick. To reduce Ni, Cu, and Co to below their detection limits, leaving only Fe particles, the sample was saw damage etched and subjected to a phosphorus diffusion gettering at 820°C for 60 min followed by a slow in-furnace cool to 600°C before removal from the furnace.

μ-XRF was performed at the Advanced Photon Source beamline 2-ID-D [12]. A 209 nm spot size at full width at half maximum and an incident photon energy of 10 keV were used to map a 16.5×15 μm^2 region with 220 nm step size. Five different effective dwell times were used: 50, 100, 250, 500, and 1000 ms. No other experimental parameters were changed

when the dwell time was changed. The maps were measured sequentially within a single eight-hour period. The effective information depth in this experimental setup for outgoing Fe K_{α} fluorescence was 8.8 μm.

All data were quantified using NIST 1832 and 1833 standards. From measurements of the standards, the theoretical minimum detection limit (MDL) for iron in the experimental setup, which is the smallest theoretically detectable elemental content, was calculated for each dwell time. The MDL is proportional to (dwell time)$^{-1/2}$. A second measure of the noise limit, the "statistical detection limit" (SDL), is defined as $\mu+4\sigma$, where μ and σ are the mean and standard deviation, respectively, of a truncated Gaussian fit to the lowest 99% of measured pixel values. See reference [3] for more details.

III. Results

Quantified synchrotron-based μ-XRF maps of the Fe K_{α} fluorescence of the same sample region are shown (Fig. 1, top row) for dwell times of 50, 250, and 1000 ms. Pixels with high Fe K_{α} fluorescence loading are black. From the maps, it is evident that for the range of dwell times studied, as the dwell time increases, more particles are detected. Additionally, many of the particles detected at all three dwell times become more prominent as the dwell time increases.

The MDL and SDL were then applied to these three maps to separate the particles from noise, and the maps were re-plotted with the detected particles in black and the noise in white (Fig. 1, bottom row). At 50 ms, 17 Fe-rich particles are identified. At 1000 ms dwell, 27 particles are identified, a 59% increase in the number of detected particles.

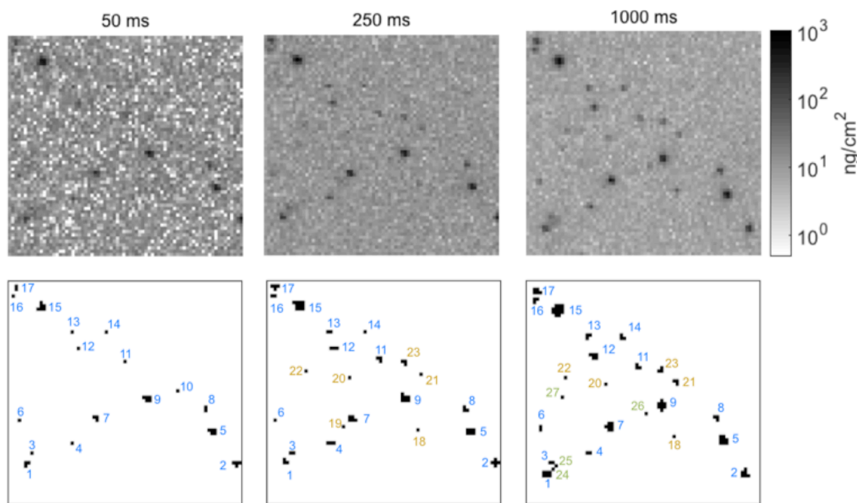

Fig. 1. μ-XRF maps of Fe K_{α} fluorescence for dwell times of 50, 250, and 1000 ms. Top row: maps of fitted, quantified area density of mass of Fe. Bottom row: binary maps highlight detected Fe particles at each dwell time that are above the minimum size limits determined by MDL and SDL. Particles are numbered, with different colors indicating detection at one (green), two (yellow), or all three (blue) dwell times. In all maps, black is high Fe loading, and white is low Fe loading.

To quantify the sensitivity as a function of dwell time, the MDL, SDL, and sizes of the detected Fe precipitates that are equal to or larger than the respective MDL were plotted for all five dwell times (Fig. 2). At longer dwell times, the two detection limits diverge, with the SDL decreasing at a slower rate as the dwell time increases. The MDL decreases from 2.2×10^5 Fe atoms/particle at a dwell time of 50 ms to 4.9×10^4 Fe atoms/particle at a dwell time of 1000 ms. The SDL decreases from 2.3×10^5 Fe atoms/particle at a dwell time of 50 ms to 8.6×10^4 Fe atoms/particle at a dwell time of 1000 ms. Particles detected with a 1000 ms dwell time, 20× longer than 50 ms dwell time, resulted in a decrease in the SDL of 63%.

The particles above both detection limits range between 2×10^5 and 2×10^6 Fe atoms/ precipitate for the 50 ms dwell time and range between 9×10^4 and 2.5×10^6 Fe atoms/ precipitate for the 1000 ms dwell time. In this experimental configuration, the 1000 ms dwell enables detection of small particles with radius between 9 and 12 nm, which the 50 ms dwell is not sensitive enough to detect.

Finally, to illustrate the new parameter space that the flyscan can access, we simulated the as-grown precipitated iron distribution for typical mc-Si with a total iron concentration of 5×10^{13} cm^{-3} and 10^{14} cm^{-3}. See [11] for further details about simulation parameters and methods. Fig. 3 shows the simulated precipitate sizes as a function of the spatial distribution of precipitates at grain boundaries and within grains. The gray area is the parameter space that was possible to scan using flyscans with 1000 ms dwell with 220 nm step size for an 8-hour scan. Highlighted in green is a region of much sparser spacing of precipitates that 50 ms dwell flyscans also with 220 nm step size for an 8-hour scan enable. Physically, this spacing of precipitates is typical of intragranular regions of multicrystalline silicon. To detect these precipitates that are more spread out, a larger region must be scanned. Compared to a 1000 ms dwell and with minor penalty on the sensitivity, 50 ms flyscans enable this larger-area scanning in the same amount of time.

These simulations show what has been born out by experience – that past observations with typical 1000 ms step scans were limited to highly-decorated grain boundaries and small clusters of intragranular dislocations. With 50 ms flyscans, while still maintaining reasonable sensitivity limits, it is now practical to map at sub-micron resolution over half a million pixels in eight hours. At a step size of 220 nm, the area that could be mapped can encompass hundreds of intragranular structural defects, which are highly detrimental to solar cell performance [13].

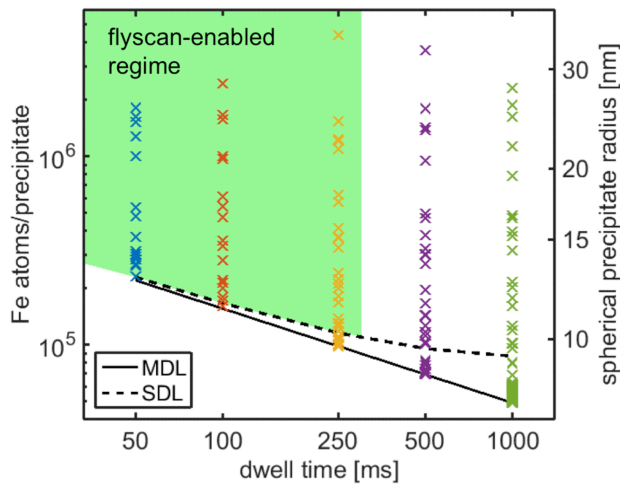

Fig. 2. The sizes of the detected precipitates compared to the MDL and the SDL at each dwell time. The green region highlights parameter space made practical by flyscans.

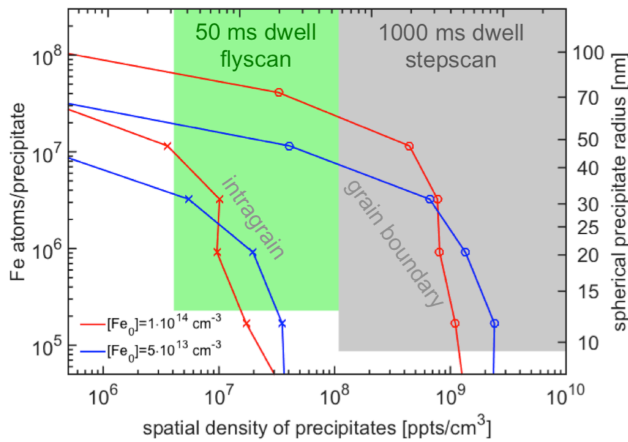

Fig. 3. New parameter space made practical with 50 ms flyscans. Simulated precipitate size vs. precipitate spatial density at grain boundaries (o's) and within grains (x's) for as-grown impurity concentrations of 10^{14} cm^{-3} (red) and 5×10^{13} cm^{-3} (blue).

IV. Discussion

Our results indicate that for the μ-XRF experimental conditions used at APS beamline 2-ID-D, if particles are larger than 2×10^5 Fe atoms, 50 ms dwell time flyscans can improve productivity by 20-fold. Either 20 times the area could be measured in a given amount of time, or one twentieth of the time would be required to map a given area. However, longer dwell times are essential for detecting smaller particles.

For precipitated impurities in mc-Si for PV, in typical material, the peak of the as-grown precipitate size distribution is around 10^4 Fe atoms/precipitate, and after a typical phosphorus diffusion, it is around 5×10^5 Fe atoms/precipitate [14]. To detect particles smaller than 10^5 atoms per precipitate, dwell times of 250 ms and higher are required while for 5×10^5 Fe atoms/precipitate, a 50 ms dwell time may be adequate.

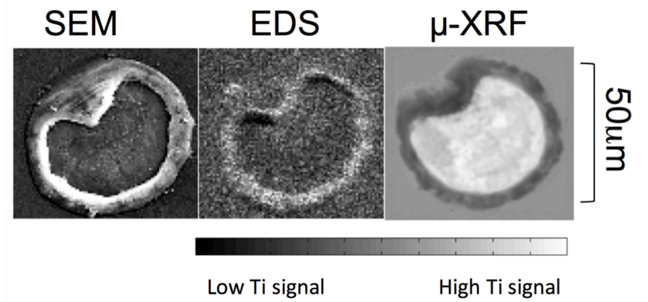

Fig. 4. Large-area correlative microscopy enabled by flyscan: titanium concentration assessment at a laser-fired contact. Sample courtesy of U. Delaware and IPG Laser.

Lastly, the faster data acquisition rate of flyscan has the potential to enable truly multi-dimensional scanning, enabling qualitatively new forms of microscopy. Examples include temperature-dependent measurements with a novel *in-situ* sample stage [15], or large-area maps to enable correlative microscopy. One example appears in Fig. 4, where the elemental distribution of titanium in a 50 μm-diameter laser-fired contact is assessed by flyscan μ-XRF in just 90 minutes; these data are correlated with scanning electron microscopy.

V. Conclusions

To fully take advantage of the new flyscan capability at APS Beamline 2-ID-D, we conducted a benchmarking study in which a region of a mc-Si wafer was characterized with synchrotron-based μ-XRF using a wide range of dwell times. Our results show that 50 ms flyscans enable a 20-fold increase in productivity without significantly sacrificing sensitivity. This quantification of the sensitivity as a function of dwell time for the accelerated data-acquistion made possible by flyscans contributes to potentially over an order of magnitude increase in productivity and enables qualitatively new forms of multi-scale microscopy at this valuable user facility.

References

[1] D. P. Fenning *et al.*, *J. Appl. Phys.* **113**, 214504 (2013)
[2] A. E. Morishige *et al.*, in *Proc. of the IEEE PVSC*, Denver, CO (2014)
[3] M. A. Jensen *et al.*, *Appl. Phys. Lett.* **106**, 202104 (2015)
[4] G. Coletti, *Prog. Photovolt: Res. Appl.* **21**, 1163-1170 (2013)
[5] D. Macdonald *et al.*, *J. Appl. Phys.* **97**, 033523 (2005)
[6] W. Shockley, W.T. Read Jr., *Physical Review* **87**, 835-842 (1952)
[7] R. N. Hall, *Physical Review* **87**, 387 (1952)
[8] S. Plekhanov, T. Y. Tan, *Appl. Phys. Lett.* **76**, 3777-3779 (2000)
[9] W. Kwapil *et al.*, *IEEE J. Photovolt.* **4**, 791-798 (2014)
[10] L. M. Murphy *et al.*, *J. Synchrotron Rad.* **2**, 64-9 (1995)
[11] A. E. Morishige *et al.*, *Appl. Phys. A* **120**, 1357 (2015)
[12] Z. Cai *et al.* in *AIP CP 521, Synchrotron Radiation Instrumentation: 11th US National Conference (AIP, Stanford, CA)*, 31–34 (1999)
[13] J. Bauer *et al. IEEE J. Photovolt.* **6**, 100-110 (2016)
[14] J. Schön *et al.*, *IEEE J. Photovolt.* **3**, 131-137 (2013)
[15] R. Chakraborty *et al.*, *Rev. Sci. Instr.* **86**, 113705 (2015)